A Letters Journal Exploring the Frontiers of Physics

November 2008

EPL, **84** (2008) 37003 www.epljournal.org
doi: 10.1209/0295-5075/84/37003

# Observation of a kink in the dispersion of f-electrons

T. Durakiewicz[1(a)], P. S. Riseborough[2], C. G. Olson[3], J. J. Joyce[1], P. M. Oppeneer[4], S. Elgazzar[4], E. D. Bauer[1], J. L. Sarrao[1], E. Guziewicz[5], D. P. Moore[1], M. T. Butterfield[6] and K. S. Graham[1]

[1] *Los Alamos National Laboratory - Los Alamos, NM 87545, USA*
[2] *Department of Physics, Temple University - Philadelphia, PA 19122, USA*
[3] *Ames Laboratory, Iowa State University - Ames, IA 50011, USA*
[4] *Department of Physics and Materials Science, Uppsala University - Box 530, S-75121 Uppsala, Sweden, EU*
[5] *Institute of Physics, Polish Academy of Sciences - 02-668 Warsaw, Poland, EU*
[6] *Lawrence Livermore National Laboratory - Livermore, CA 94550, USA*

received 10 July 2008; accepted in final form 15 September 2008
published online 15 October 2008

PACS 79.60.-i – Photoemission and photoelectron spectra
PACS 71.28.+d – Narrow-band systems; intermediate-valence solids
PACS 74.25.Jb – Electronic structure

**Abstract** – Strong interactions in correlated electron systems may result in the formation of heavy quasiparticles that exhibit kinks in their dispersion relation. Spectral weight is incoherently shifted away from the Fermi energy, but Luttinger's theorem requires the Fermi volume to remain constant. Our angle-resolved photoemission study of $USb_2$ reveals a kink in a noncrossing $5f$ band, representing the first experimental observation of a kink structure in $f$-electron systems. The kink energy scale of 21 meV and the ultra-small peak width of 3 meV are observed. We propose the novel mechanism of renormalization of a point-like Fermi surface, and that Luttinger's theorem remains applicable.



**Introduction.** – Since the remarkable discovery of heavy-fermion superconductivity in $CeCu_2Si_2$ [1], the properties of $f$-electron materials were linked to the renormalization of electron effective masses due to strong electronic correlations. At low temperatures, a typical heavy-fermion system behaves as a Fermi liquid with heavy quasiparticles, while, at higher temperatures, it exhibits a local moment character. The cross-over between these two types of behavior is driven by the high entropy associated with the local moments that is removed at low temperatures when the electrons delocalize leading to the formation of the heavy Fermi liquid. Hence, the $f$-electrons exhibit a dual nature, and the physical properties of $f$-electron systems become sensitive to minute changes in parameters like temperature, pressure, magnetic field etc., exhibiting a plethora of exotic and often coexisting states. Details of the quasiparticle mass renormalization are central to understanding these properties.

In the low-temperature electronic structure of strongly correlated $d$-electron systems, electron correlations may lead to band renormalization. Narrow, dispersive quasiparticle bands are formed in the vicinity of the Fermi energy, exhibiting long lifetimes and increased effective masses. Numerous studies have been recently directed at a detailed spectral analysis of the quasiparticle dispersion in strongly correlated systems, especially in the high-temperature superconductors. This effort revealed the existence of characteristic energy scales, or kinks, in the quasiparticle excitation spectrum. The observed kink energy scales range from 40 meV [2] in high-temperature superconductors up to 900 meV [3] in graphene. The nature of kink-like changes in the slope of band dispersion is being vigorously debated. Kinks are taken as evidence for the coupling of electrons to either phonons or spin fluctuations [4–8]. Multiple coexisting energy scales were reported for kink-like many-body interaction effects in cuprates [9]. Recently it was also proposed that within a coupling-free scenario [10], kinks emerge solely from electron correlations. Spectroscopic evidence for the first two mechanisms is found in the $d$-electron high-temperature superconductors, but no kink structures have been observed in $f$-electron systems. Here we describe the first observation of a kink in the $5f$ quasiparticle excitation spectrum obtained by high-resolution angle-resolved photoelectron spectroscopy (ARPES), linked to the local spin density approximation (LSDA) band structure

(a) E-mail: tomasz@lanl.gov

and many-body calculation. Contrary to the previously reported observations, we find a kink in a band that does not cross the Fermi level. Within the renormalized region we find the $5f$ quasiparticle intrinsic peak width of less than 3 meV, the narrowest ever observed in the photoemission of $f$-electrons. We propose a novel mechanism of renormalization of a point-like Fermi surface to explain our findings.

Uranium dipnictides $UX_2$ (X = P, As, Sb and Bi) are a family of correlated $f$-electron antiferromagnets with tetragonal structure ($P4/nmm$) which have relatively high Néel temperatures [11,12] and complex transport properties [13]. The electronic specific heat of $USb_2$ of 25 mJ K$^{-2}$ mol$^{-1}$ is small in comparison with Ce-based heavy fermions, but is typical for many uranium compounds where strong hybridization between $5f$ and conduction electrons leads to itinerant behavior. In recent years, extensive de Haas - van Alphen (dHvA) work revealed cylindrical sections of the Fermi surface of quasi–two-dimensional character [14–16] with axes parallel to the [001] direction. The itinerant nature of $5f$-electrons is reflected in the large cyclotron masses inferred from the dHvA oscillations which range from $1.84m_0$ to $8.33m_0$, depending on the sheet of the Fermi surface [17]. A $5f$ contribution to the conduction band was derived from these observations. Early photoemission studies [18] revealed the dispersive nature of the $5f$ bands and confirmed the quasi–two-dimensional character of $USb_2$. More recently, high-resolution angle-resolved photoemission was used to measure the dispersions of the $5f$ band near the Fermi level [19]. A dispersion of at least 14 meV was found along the $\Gamma$-$X$ direction, and less than 10 meV in the $\Gamma$-$Z$ direction, with the line width less than 10 meV. In the present work we establish the line width to be no larger than 3 meV in some parts of the band.

**Experiment and theory.** – The risk of radioactive contamination of expensive high-resolution photoelectron spectrometers and synchrotron storage rings is a limiting factor in the arena of actinide research. Importantly for photoemission techniques, $f$-electron materials are also very susceptible to surface contamination by residual gases which are always present in a vacuum measurement chamber. High-quality single crystals and ultra-high vacuum conditions are therefore essential. In our experiments, we use high-quality, flux-grown single crystals cleaved *in situ* in an ultra-high vacuum environment. The $USb_2$ sample ordered antiferromagnetically below the Néel temperature of 205 K, as indicated by our susceptibility measurements. The ordered moment is about $1.8\mu_B/U$. The crystal orientation was determined by X-ray diffraction prior to measurement. The base pressure in the measurement chamber did not exceed $3 \times 10^{-11}$ torr. Angle-resolved photoemission was performed using the Plane Grating Monochromator beamline at the synchrotron Radiation Center in Stoughton, Wisconsin. We used 34 eV photons, with an overall energy resolution better than 20 meV and an acceptance angle of $\pm 1$ degree. In the tetragonal layered $Cu_2Sb$-type structure, with $c/a$ ratio equal to 2, an easy-cleave plane exists parallel to the $\vec{a}$ direction. Measurements were performed at a temperature of 15 K and the data were normalized to a Pt Fermi level reference. Peak spectral properties were established by nonlinear multiparameter regression fitting of the experimental data for each $k$ value with a convolution of Fermi function, a Gaussian width representing the energy resolution and an asymmetric Doniach-Sunjic (DS) width representing the intrinsic lifetime (see the appendix for more details). The DS picture is commonly used for valence band and near-EF quasiparticle features as a tool for describing asymmetry [20,21]. This is implemented here in terms of the asymmetric variation in the Lorentzian component of the fit. The real part of the self-energy function was found self-consistently by a Kramers-Kronig transformation of the measured spectrum.

The density functional theory (DFT) calculations presented here for $USb_2$ were performed using the full potential local orbitals (FPLO) method [22], adopting the local spin density approximation (LSDA). In our fully relativistic, full-potential calculations, the $f$-electrons were treated as itinerant and included in the set of valence states. The antiferromagnetic superstructure of $USb_2$ was assumed in the calculations, adopting the experimental lattice parameters $a = 4.27$ Å and $c = 8.748$ Å. The following basis sets were assumed for U and Sb: $6s6p6d; 7s7p$ and $5f$; and $4s4p4d; 5s5p$, respectively. The Perdew-Wang parametrization [23] of the LSDA exchange correlation energy was adopted in our calculations.

In order to test our LSDA calculation the optimized theoretical volume (at minimum total energy) was calculated to be 1.2 percent smaller than the experimental volume.

Finally, many-body calculations were performed which incorporated the coupling between the electronic bands and the spin fluctuations of the antiferromagnetic state. The real part of the self-energy yields a renormalization of the quasiparticle dispersion relation due to the mass enhancement, while the imaginary part is responsible for the peak width. These calculations only take into account two bands which are split due to the antiferromagnetic order; one of which is completely filled and a second band which crosses the Fermi energy. Due to the difference in the LSDA band dispersion relations of these two bands, electrons in these bands have different self-energies even when interband scattering processes are taken into account. The shift in the Fermi energy due to the many-body interactions is obtained directly from the self-energy of the band which crosses the Fermi energy. The angle-resolved spectrum was calculated from the imaginary part of the one-electron Green's function. The Green's function was calculated using the LSDA bands and a $k$-dependent self-energy which incorporated boson emission and absorption processes. The bosons were

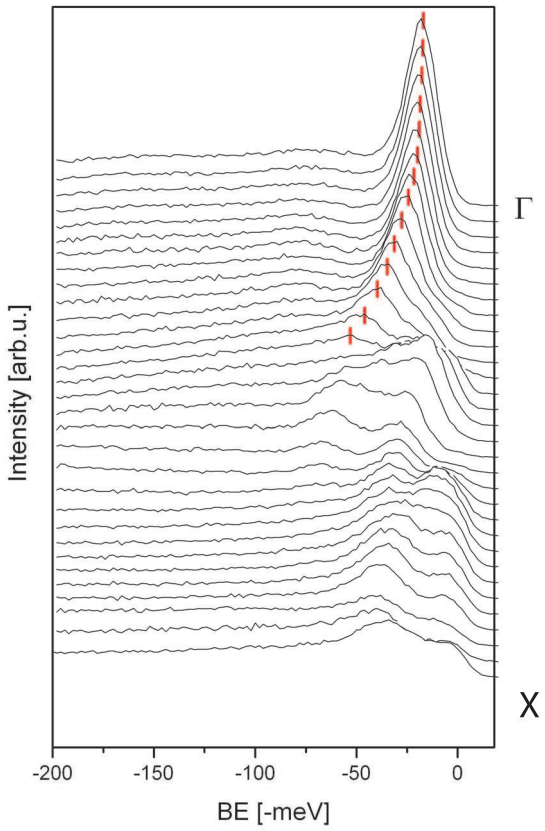


Fig. 1: (Colour on-line) Electronic structure of $USb_2$ along the Γ to $X$ direction. Angular scans between Γ (top of the picture) and $X$ points in the Brillouin zone of $USb_2$ are shown, with photoemission intensity normalized only to mesh current, *i.e.* photon beam intensity. Data were taken at a photon energy of 34 eV. Red markers indicate the quasiparticle peak binding energy obtained from nonlinear fitting (see text for explanation) for the band discussed here.

modeled by a Debye spectrum, and the vertex corrections were ignored, in accordance with Migdal's theorem [24,25].

**Results.** – A detailed view of the ARPES spectra along the Γ-$X$ direction of the Brillouin zone is presented in fig. 1. The Fermi level is marked "0", and the binding energy scale is 200 meV. The spectra presented in fig. 1 reveal that the dominant feature is a single band "A", indicated with red markers, which disperses towards higher binding energies. Several crossing bands corresponding to cylindrical Fermi sheets found in dHvA appear around and above the mid-zone area, but are of much weaker spectral weight than band A. Both our previous Fano resonance measurements [19] and our current DFT band structure calculation indicate that the narrow near-Fermi energy ($E_F$) features are predominantly of $5f$ character. These features are strongly renormalized, which leads to the extremely narrow natural line width. A direct comparison of the LSDA band structure calculations and measurements is shown in fig. 2. Both the LSDA calculation and the high-resolution

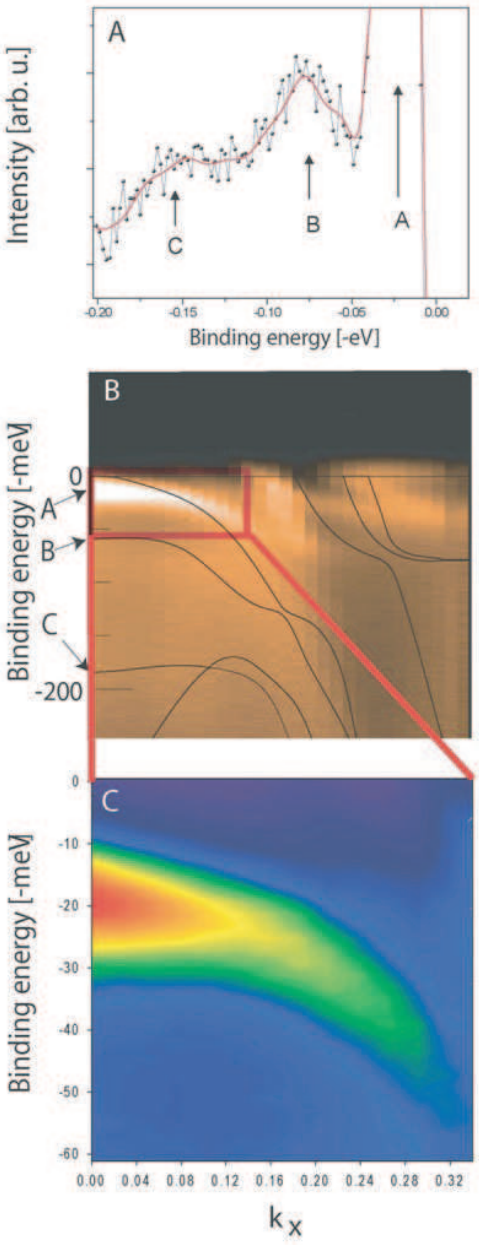


Fig. 2: (Colour on-line) Details of the electronic structure of $USb_2$ and comparison with LSDA calculation. Panel A) shows the energy distribution curve (EDC) in the vicinity of the Γ point, with intensity enhanced to show the B and C bands clearly. Bands A, B and C are marked with arrows. The contour plot of the EDCs between Γ and $X$ points is shown in panel B), with the characteristic features A, B and C marked the same as in panel A). The calculated LSDA band structure is also shown in panel B) in black lines. Relatively good agreement is obtained between LSDA band positions A, B and C along the high symmetry point (Γ). However, when moving towards the $X$ point, one can clearly notice discrepancies: the measured band dispersion is flattened in comparison to LSDA. The flattening of bands appears within the first 20–50 meV below the Fermi level. Panel C) shows the focus of our attention in this paper, namely the expanded view of the quasiparticle band A dispersing from the zone center, with a clearly visible kink in the middle part of this panel.

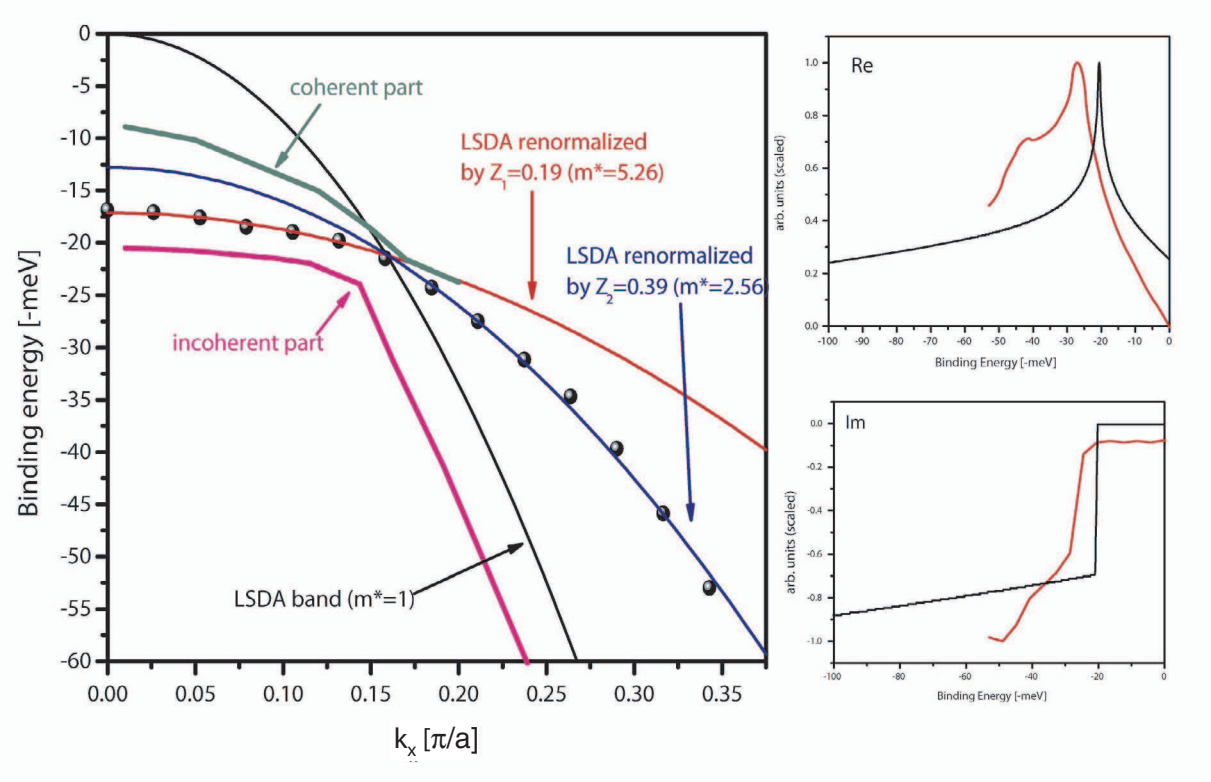


Fig. 3: (Colour on-line) Dispersion and spectral function properties of band A. Two distinct renormalization regions may be seen here, separated by a kink. The LSDA band is plotted in black, whereas the two renormalization regions $Z_1$ and $Z_2$ are in red and blue, respectively. Each black dot corresponds to the peak position found by the nonlinear multiparameter regression fitting of a single EDC scan for a given momentum value. If we denote the measured band dispersion as $\epsilon_{EXP}$, and use the LSDA band dispersion $\epsilon_{LSDA}$ as a bare band analogue, then a renormalization factor $Z$ may be found by comparing the slope of $\epsilon_{EXP} = Z\,\epsilon_{LSDA}$. In order to match the experimental dispersions, we have renormalized the original LSDA band by the factor $Z_1 = 0.19$ in the binding energy ($E_B$) - momentum ($k_x$) space of ($-20 < E_B < 0$, $0 < k_x < 0.18$), and factor $Z_2 = 0.39$ in ($-60 < E_B < -20$, $0.18 < k_x < 0.35$) space, where the energy is in $-$meV and the momentum in $\pi/a$ units, respectively. The kink appears near $E_B = -20$ meV and $k_x = 0.18$, as the separation of two different regions of renormalization. Interestingly the directions of the $Z_1$ and $Z_2$ shifts are opposite, and band A seems to align with the LSDA band at energies below 150–200 meV, but the spectral intensity in this region is too low to clearly identify such alignment. The real and imaginary parts of the self-energy are shown in the right-hand panels (black lines), together with measured values (red lines).

ARPES measurements show features corresponding to the bands A, B and C, shown in fig. 2 for $k = 0$ in panel A). We will now focus on the properties of the strongest band A, shown in panel B) and enhanced in panel C), where owing to high intensity we can determine spectral properties accurately. Interesting differences in the dispersion of band A are found between the LSDA calculation and the experiment. Particularly, the abrupt changes in the band dispersion brought in by renormalization are not reproduced in the LSDA calculation, which lacks strong electron correlations and coupling to bosonic fields. We have therefore performed the many-body calculations where the electronic correlations are introduced in the form of low-energy bosonic excitations. The renormalization of band A is shown in detail in fig. 3, where the binding energy of band A is shown as a function of momentum. Two distinct regions of $k$-space may be seen here, separated by a kink in the dispersion relation. Our many-body calculation result is also shown in fig. 3, as well as a comparison of the measured and calculated real and imaginary parts of the spectral function. Both real and imaginary parts are in good agreement with calculations.

The limits of the angular resolution might contribute to a smooth transition towards increasing peak width, if the analysis were performed on a strongly dispersive band. Band A is only slightly dispersive, and the observed changes in the peak width are rapid and associated with the kink energy scale, therefore may not be explained by resolution effects. We conclude that the observed kink structure, as manifested in binding energy, peak width and peak asymmetry, is not an artefact of data reduction.

The spectroscopic details of the kink: dispersion, asymmetry, lifetime and peak width are shown in fig. 4. The asymmetry parameter, fitted in the sense of Doniach-Sunjic asymmetry, indicates a clear boundary between the two regions. We find the corresponding increase in asymmetry for small $k$ in our many-body calculations. For the completely filled band, a final-state hole with Bloch wave

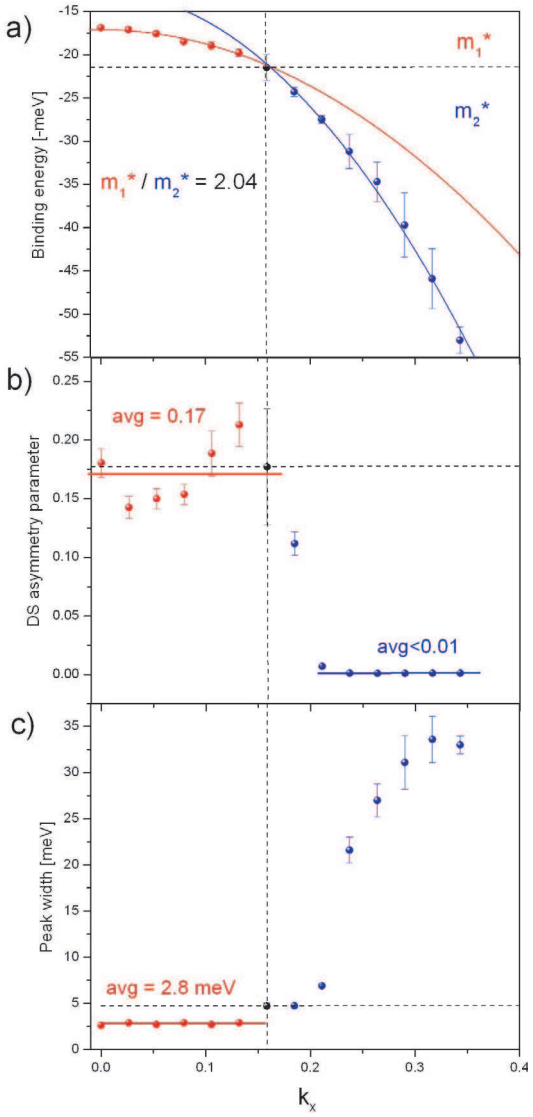


Fig. 4: (Colour on-line) Spectroscopic details of the kink. Red and blue dots represent experimental values. The band dispersion in two renormalization regions indicated in red and in blue, respectively, is shown in panel a). The corresponding dispersion fits are $\epsilon = -17.13\,\text{meV} - 162.38k_x^2$ and $\epsilon = -12.77\,\text{meV} - 331.03k_x^2$ for red ($Z_1$) and blue ($Z_2$) parabola, respectively. Hence, the effective quasiparticle masses $m_1^*$ and $m_2^*$ for $Z_1$ and $Z_2$ regions, respectively, are calculated from curvatures, and the ratio $m_1^*/m_2^*$ is found to be close to 2. The Doniach-Sunjic asymmetry parameter and peak width are shown in panels b) and c), respectively. In each plot a distinct boundary between two renormalization regions may be noted.

vector $\underline{k}$ can decay to states with wave vector $\underline{k}-\underline{q}$ by the emission of a low-energy bosons with wave vector $\underline{q}$. This intraband decay process contributes to the low binding energy tail of the ARPES peak when $\varepsilon_{\underline{k}-\underline{q}} > \varepsilon_{\underline{k}}$. However, because of the inverted nature of band A, there is limited phase space available for this process when $\varepsilon_{\underline{k}}$ is close to the top of the band and so the peak becomes asymmetric.

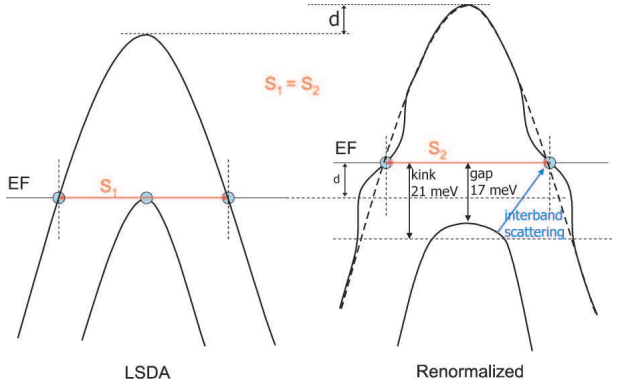


Fig. 5: (Colour on-line) Renormalization of the point-like Fermi surface. $S_1$ and $S_2$ represent the Fermi volume before and after renormalization, respectively, and EF is the Fermi level. LSDA bands (left panel) are renormalized in a way that induces as flattening of the band and a shift in the Fermi energy. Two combined effects result in the formation of a kink structure at an energy scale of 21 meV and a gap of 17 meV, while Luttinger's condition of $S_1 = S_2$ is maintained.

A dramatic transition may also be seen in fig. 4 in the peak width and corresponding lifetime. The peak width of less than 3 meV in the $Z_1$ region is an order of magnitude smaller than the binding energy and corresponds to a quasiparticle lifetime of over 200 fs. The ultra-small width shows up in our many-body calculations for small $k$, where the quasiparticle peak breaks off from the continuum spectra and becomes a delta function, similar to the situation found by Engelsberg and Schrieffer [26] for a band which crosses the Fermi energy. However, on extending their analysis to noncrossing bands, one finds a zero-width quasiparticle peak without a kink. This finding is in accordance with measurements on semiconductors [27], but insufficient in explaining the kink structure in $USb_2$.

**Discussion.** – We propose that the maximum of the LSDA band in $USb_2$ has a single common point with the Fermi energy, but the measured band A is renormalized and shifted 17 meV below the Fermi energy. This presents a novel and exciting situation in which the Fermi liquid theory is pushed to the extreme for the point-like Fermi surface, as shown in fig. 5. The Fermi surface is usually defined in terms of a discontinuity of the momentum distribution of electrons $n_k$. Luttinger [28] proved that the volume enclosed by the Fermi surface is independent of the strength of the interactions. In the normal state of the quasi–two-dimensional high-$T_c$ superconductors, the Fermi liquid concept prevails even when the discontinuity in $n_k$ becomes small due to the vanishing of the quasiparticle weight [29]. In our case, the discontinuity occurs at an isolated point so Luttinger's theorem may be called into question. Furthermore, renormalized quasiparticle masses and enhanced lifetimes are not expected in noncrossing bands, so the applicability of the quasiparticle concept may also be questioned. However, when

interband transitions involving a band which crosses $E_F$ are taken into account, then our many-body calculations indicate that a kink is induced into the dispersion relation of the noncrossing band. Due to the difference in the self-energies of the crossing band and the noncrossing band, the Fermi energy is renormalized upward by the electron-boson scattering. The band forming a point-like Fermi surface is pushed down, thereby removing any cause for a violation of Luttinger's theorem.

Even though band A in $USb_2$ starts at 17 meV below the Fermi energy, the spectrum associated with this band still shows properties of a renormalized Fermi liquid, such as the kink in the dispersion relation and ultra-sharp quasiparticle peaks. These features may be assigned to interband electron-boson scattering processes, with asymmetry being controlled by intraband scattering. We show, for the first time, the existence of a kink structure in $f$-electron materials. Our findings extend the kink physics from $d$-electron to $f$-electron arena, where the high-resolution spectroscopy methods of analyzing the spectral function still have to play their role, hopefully leading to breakthroughs similar to those observed in unconventional superconductors within the last decade.

* * *

This work was performed under the auspices of the U.S. DOE and LANL LDRD Program. The SRC is supported by the NSF under Award Np. DMR-0084402. Support from the Swedish Research Council (VR), SNIC, and European Commission (JRC-ITU) is gratefully acknowledged. Thanks are due to K. Byczuk, A. Kaminski, J. D. Thompson, F. Ronning, T. Klimczuk, C. Batista, A. Balatsky and Y.-F. Yang for stimulating discussions. EG was supported by the Polish grant N202 140 32/3877.

## Appendix

High fit quality is achieved through the use of a numerical procedure based on minimizing the sum of the squares of $M$ nonlinear functions in $N$ variables by a modification of the Levenberg-Marquardt algorithm. We have obtained convergence with the average chi-square value of 0.03 for about 1000 to 4000 iterations depending on $k$, which corresponds to a very good fit. The core of the solver was developed at the Sandia National Laboratory in 1981–1986 on the basis of earlier codes from the Argonne National Laboratory. This core was used as engine for our own code written about 20 years ago by one of us [30], where the Doniach-Sunjic lineshape in the valence band context is modelled by a convolution of Gaussian, Lorentzian, Fermi function at temperature, DS asymmetry, background and branching ratio with spin-orbit splitting for shallow core-levels fitting (not used here). We start the fitting with the $k = 0$ curve, where the initial binding energy of the three peaks A, B and C shown in panel A) in fig. 2 is taken from the LSDA band structure; then the solver converges to peak A being below the Fermi level, while peaks B and C converge in good agreement with LSDA. Subsequently, the values for all parameters obtained for the converged $k = n$ fit are used as starting values for the next $k = n + 1$ fit. The error of the mean is decreasing with a square root of the number of samples. In other words, it is very well known in spectroscopy that a peak position can be determined with an accuracy better than the experimental resolution if a sufficient number of points is available per peak. Here, the problem of error propagation is more complex due to nonlinear fitting, but the error values may be obtained for a diagonal of the covariance matrix or from a Monte Carlo error propagation analysis. Our analysis is based on approximately 150 experimental points per scan. As may be seen in fig. 1 the binding energy of the quasiparticle peak does not always correspond exactly to the maximum intensity. The quasiparticle peak binding energy is in fact convoluted, hence the de-convolution process through the above-described fitting must be performed for each $k$.

## REFERENCES

[1] Steglich F. *et al.*, *Phys. Rev. Lett.*, **43** (1979) 1892.
[2] Cuk T. *et al.*, *Phys. Rev. Lett.*, **93** (2004) 117003.
[3] Bostwick A. *et al.*, *Nat. Phys.*, **3** (2007) 36.
[4] Lanzara A. *et al.*, *Nature*, **412** (2001) 510.
[5] Shen Z. X. *et al.*, *Philos. Mag. B*, **82** (2001) 1349.
[6] Johnson P. D. *et al.*, *Phys. Rev. Lett.*, **87** (2001) 177001.
[7] Kaminski A. *et al.*, *Phys. Rev. Lett.*, **86** (2001) 1070.
[8] Damascelli A., Hussain A. and Shen Z.-X., *Rev. Mod. Phys.*, **75** (2003) 473.
[9] Meevasana W. *et al.*, *Phys. Rev. B.*, **75** (2007) 174506.
[10] Byczuk K. *et al.*, *Nat. Phys.*, **3** (2007) 168.
[11] Trzebiatowski W. and Troc R., *Bull. Acad. Pol. Sci. Ser. Sci. Chim.*, **11** (1963) 661.
[12] Henkie A. and Kletowski Z., *Acta Phys. Pol. A*, **42** (1972) 405.
[13] Wawryk R., *Philos. Mag.*, **86** (2006) 1775.
[14] Aoki D. *et al.*, *Philos. Mag. B*, **80** (2000) 1517.
[15] Wisniewski P. *et al.*, *J. Phys. Soc. Jpn.*, **70** (2001) 278.
[16] Aoki D. *et al.*, *Physica B: Condens. Matter*, **281** (2000) 761.
[17] Aoki D. *et al.*, *J. Phys. Soc. Jpn.*, **68** (1999) 2182.
[18] Arko A. J. *et al.*, *Philos. Mag. B*, **75** (1997) 603.
[19] Guziewicz E. *et al.*, *Phys. Rev. B*, **69** (2004) 045102.
[20] Casey P. A. *et al.*, *Nat. Phys.*, **4** (2008) 210.
[21] Joyce J. J. *et al.*, *Phys. Rev. B*, **54** (1996) 17515.
[22] Koepernik K. and Eschrig H., *Phys. Rev. B*, **59** (1999) 1743.
[23] Perdew J. P. and Wang Y., *Phys. Rev. B*, **45** (1992) 13244.
[24] Migdal A. B., *Sov. Phys. JEPT*, **7** (1958) 996.
[25] Wojciechowski R. J., *Physica B: Condens. Matter*, **259-261** (1999) 498.
[26] Engelsberg S. and Schrieffer J. R., *Phys. Rev.*, **111** (1963) 993.
[27] Jiménez I. *et al.*, *Phys. Rev. B*, **56** (1997) 7215.
[28] Luttinger J. M., *Phys. Rev.*, **119** (1960) 1153.
[29] Varma C. M. *et al.*, *Phys. Rev. Lett.*, **63** (1989) 1996.
[30] Joyce J. J. *et al.*, *J. Electron. Spectrosc. Relat. Phenom.*, **49** (1989) 31.